THE VARIATION OF THE VICKERS MICRO-HARDNESS IN THE VICINITY OF THE FRACTURE SURFACES AT STATIC LOADING

GOANTA VIOREL [*], AXINTE TOADER, IFTIMIE DUMITRU GEORGE

Technical University "Gheorghe Asachi" Iaşi, Bd. Mangeron, nr. 67, 700050 Iaşi, Romania

Abstract: The paper presents an experimental and analytical process aimed at establishing correlations between the hardness value and the level of plastic deformation. In these conditions, static tensile tests were performed on the compact specimen. These tests allowed us to determine the K_{Ic} fracture toughness, as well as to obtain surfaces generated by the material fracture. In the vicinity of the fracture surfaces, Vickers micro-hardness tests were also performed. Two types of determinations were utilized for normal OLC45 steel and for the annealed OLC45 steel. Significant differences regarding the Vickers values were observed; they were determined by the differences which appeared around the crack.

Keyword: plastic deformations, Vickers micro-hardness, fracture toughness.

1. INTRODUCTION

When a part fails, significant plastic deformations appear in the vicinity of the fracture surfaces. The level of plastic deformations in these areas depends on the characteristics of the material and the type of loading. It is a known fact that the level of plastic deformation may be correlated to the value of the micro-hardness determined in the plastic deformed area.

The continuous functioning for a long time, in certain loading and environmental conditions, may affect (more or less) the strength characteristics and fracture toughness of the materials various components are made of. For the devices currently running, there are few tests able to determine the level of plastic deformation which appears as a consequence of previous loadings. Some of them are: the determination for residual stresses, defectoscopic methods, x-ray diffraction and methods based on photo-elasticity etc. We proposed this type of method in the present paper, in order to establish a correlation between the level of plastic deformation (caused by the loading at various conditions) and the Vickers hardness number determined on the parts. Based on these tests, we ca assess the remaining life time of the parts, components, structures. The advantages of such tests are: simplicity, low-cost, and the fact that the parts loaded at Vickers micro-hardness don't suffer damages which might affect their integrity [1]. It is obvious that the determinations of the "in situ" micro-hardness have to be preceded by lab tests for each material. This way, the correlation between the plastic deformation and the micro-hardness should be obvious. This method is based on the fact that, after the yield stress is exceeded, it strengthens in its volume and therefore changes its hardness. Hardness tests have been for a long time a standard method for material characterization as they provide an easy, inexpensive, non-destructive and objective method of evaluating basic properties from small volumes of materials. As well as resistance to plastic deformation; stiffness, residual stresses near the surface, and the fracture toughness of the material are some basic properties that can be evaluated by the hardness tests [2].

[*] Corresponding author, e-mail: vgoanta@tuiasi.ro
© 2011 Alma Mater Publishing House

In the literature, Vickers hardness number (HV) has been the most popular in the investigation of the relationship between hardness and the lifetime or tensile strength of the material because of two reasons: firstly, its superior resolution as compared to spherical indenters; and secondly, the Vickers indenter is self-similar, through which the hardness is ideally independent of the indentation load and indentation depth. Therefore, in this study, Vickers indentation will be as well the main concern. A basic review of the first results is covered by Tabor [3]. Tabor has shown that the mean contact pressure P_m (or hardness) can be related to the yield stress σ_y or tensile strength R_m of the material, by an expression based on the theory of indentation of rigid-perfectly plastic solid:

$$HV = \frac{\text{Indenter Force (kgf)}}{\text{Imprint Surface Area (mm}^2\text{)}} \tag{1}$$

For non-strain hardening materials, the Vickers hardness number, which is defined as in the above formula, can be related to the constant yield stress, σ_y, by:

$$HV = (2.9 \div 3.0) \quad \sigma_y \tag{2}$$

For strain hardening materials and on empirical bases, Tabor suggests to be used a similar expression as in the case of non-strain hardening materials, but using as yield stress the value that corresponds at a representative plastic strain:

$$HV = 2.9 \cdot \sigma_y \ (at\ an\ engineering\ \ plastic\ strain\ of\ \ 0.08) \tag{3}$$

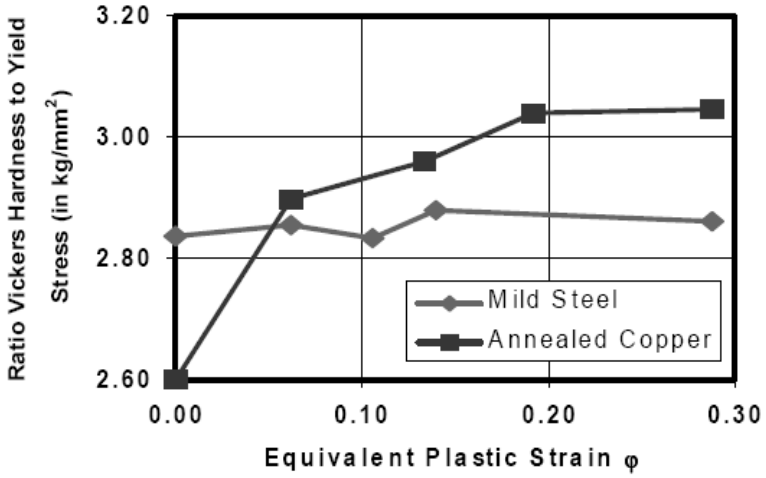

Fig. 1. Experimentally determined Vickers Hardness Number and Yield Stress ratios for various amounts of initial plastic strain.

Figure 1 shows a comparison of Tabor's formula with his own experimental results. In this plot, φ□ designates the ***equivalent true plastic strain,*** experienced by the specimen before indentation [4]. It can be observed that the agreement is rather good for mild steel, whereas for the annealed copper a scatter of about 15% is present. It should be emphasized that Tabor's formula is given at various places with slightly varying coefficients and representative strain values, as compared with the values that are given in Eqn.3.

The relationship between Vickers hardness number and yield stress, as related to metal forming, is investigated by Dannenmann and Wilhelm [5].

The experimental results can be seen in Figure 2. In their original work, no use of Tabor's model as explained above was made, so that an interpretation of their experimental results utilizing Tabor's model is also given in this figure. However, even this improved curve indicates a conversion error of about 20%.

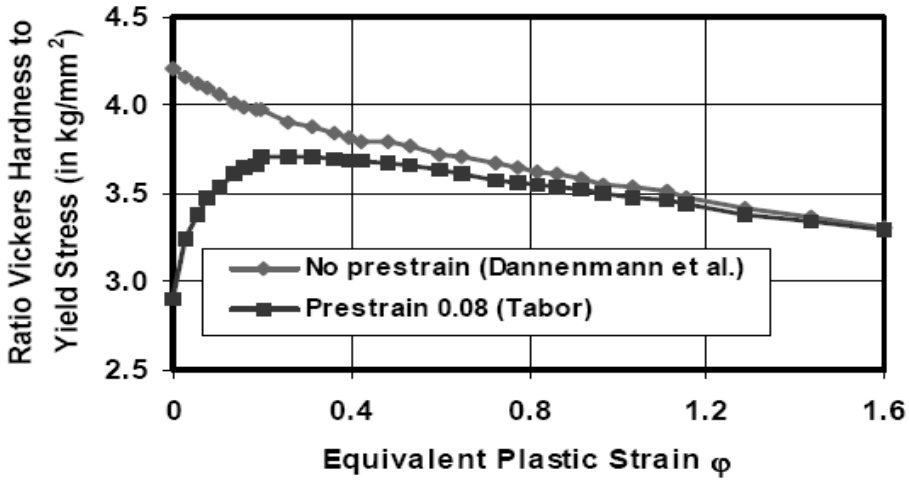

Fig. 2. Ratio of Vickers Hardness Number and Yield Stress, by Dannenmann and Wilhelm [5].

As an observation based on the above-cited researches, it can be said that the experimental studies lack the separation of various factors affecting the hardness and lifetime or tensile strength relationship. On the other hand, the analytical and numerical studies lack either quantitative accuracy and/or they don't cover metal-forming issues properly.

2. DETERMINATION OF MECHANICAL AND ELASTICALLY CHARACTERISTICS OF MATERIALS

As we already mentioned, for fabrication of compact samples, both normal OLC45 steel and temperature-annealed OLC45 steel were used. The characteristic stress-strain curves for both materials are presented in Figure 3. These curves, as well as the mechanical characteristics, were determined in a laboratory based on tensile tests performed on the universal testing device INSTRON 8801.

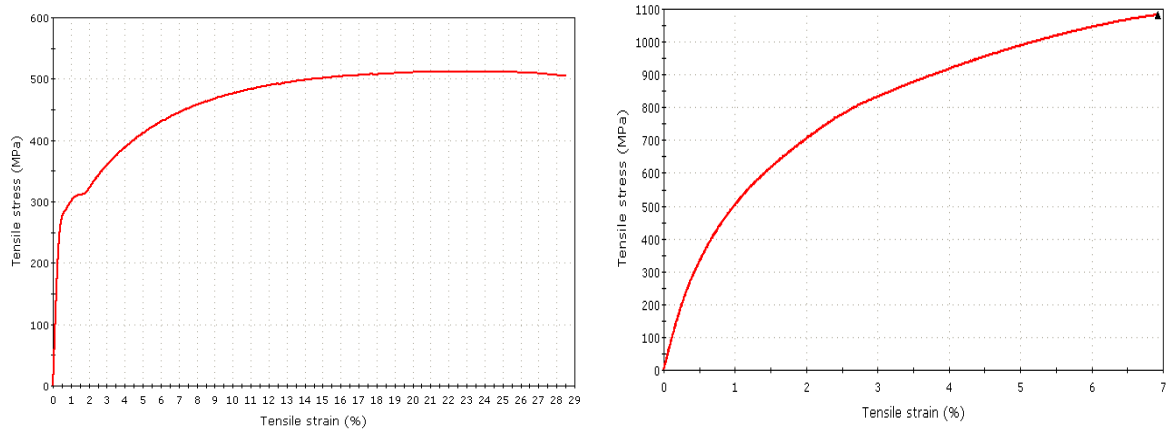

a) OLC45; b) OLC45 annealed

Fig. 3. Characteristic stress-strain curve.

Important differences are observed regarding the allure of the curves, especially after they go beyond the elastic domain. The mechanical characteristics required for the software of Fracture Mechanics in order to determine K_{Ic} are: ultimate tensile strength, yield limit, Young modulus and Poisson coefficient, [6]. The first two characteristics were given by the testing device:

$R_{m\text{-}OLC45}$=511 MPa; $R_{m\text{-}OL45\text{-}annealing}$=1055 MPa; $\sigma_{c\text{-}OLC45}$=275 MPa; $\sigma_{c\text{-}OLC45\ annealing}$=470 MPa.

The appearance of the fracture surfaces of the two specimens can be seen in Figure 4. We observed that, while normal OLC45 steel presents a bottleneck effect at fracture, the annealed OLC45 broke on a perpendicular surface on the loading direction with no visible bottleneck. As a consequence, the annealed OLC45 has certain fracture fragility.

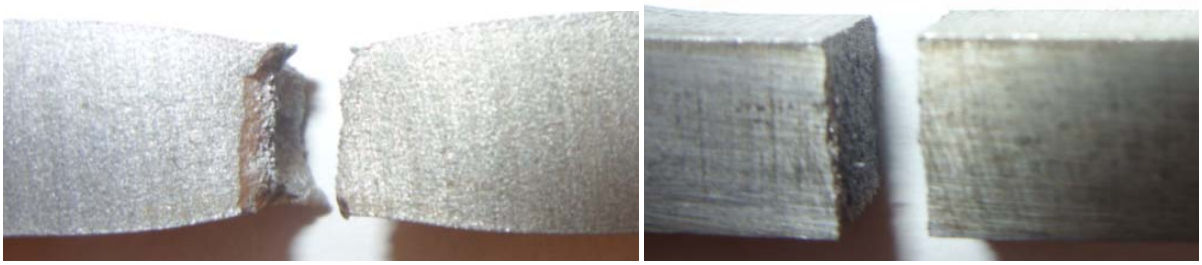

a) OLC45; b) OLC45 annealed

Fig. 4. The appearance of the fracture surfaces for the plain specimens loaded in tension.

In order to determine the Young modulus and Poisson coefficient, the method we used was to apply strain gauges in T-shape, on the longitudinal and transversal direction of the plain specimens in the elastic domain, Figure 5. In order to acquire the signal from the gauges, we used a Vishay P3 tensiometric bridge, which exports a data file containing the values of the specific deformations on longitudinal (ε_l) and transversal (ε_t) directions. A file containing data with values for force, time, stress etc. has also been imported from the testing device. By comparing the two files and eliminating the time parameter, a data table containing values for stress σ and the two specific deformations on longitudinal and transversal directions is obtained. The slope of the curve (drawn in σ-ε_l coordinates) represents the Young modulus in the points obtained from the two files. The slope of the drawn curve in ε_t-ε_l coordinates represents the Poisson coefficient. The values for the two elastic characteristics were:

E-OLC45=1.97·105 MPa; E-OL45-annealing=1.90·105 MPa; ν-OLC45=0.268; ν-OLC45 annealing=0.271.

Fig. 5. Strain gauge in T-shape apply on the plain sample.

3. THE EXPERIMENTAL DETERMINATION OF THE FRACTURE TOUGHNESS

The experimental determination of the fracture is standardized by ASTM E 399/1997 and refers to specimens made of metallic materials with a linear-elastic behavior until fracture [7]. The purpose of the test is the determination of the critical value of the intensity factor of the K_{Ic} stress in plane status deformation conditions. This method involves testing standardized samples, with an initial lateral notch and a crack propagated by fatigue further on, Figure 6. The pre-fracture through fatigue happens due to the cyclical loading of the notch sample, with a ratio between the minimum and maximum stress that would lead to an asymmetrical coefficient of the cycle located in the interval 1 ÷ 0.1. The specimens used for the tests had a B=25 mm thickness and a W=62.5 mm width.

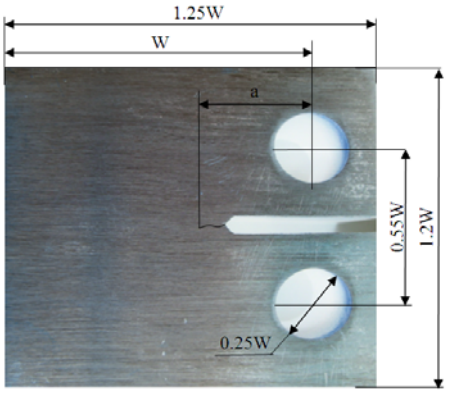

Fig. 6. The compact sample used to determine KIc.

We used the "K_{Ic}" program, installed on the PC controlling the testing device INSTRON, in order to load the compact specimen at tensile, with a crack propagated by fatigue. In the program, certain parameters should be given, such as the dimensions of the compact sample, the "a" length of the crack, the mechanical and elastically characteristics of the material, the loading speed, etc., [8]. Figure 7 presents the variation graphs of the loading force compared to the displacement of the crack side, measured using a "clip-on-gage" extensometer.

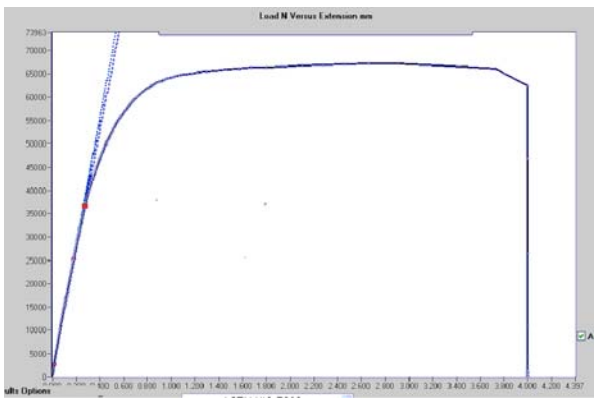

a) OLC45

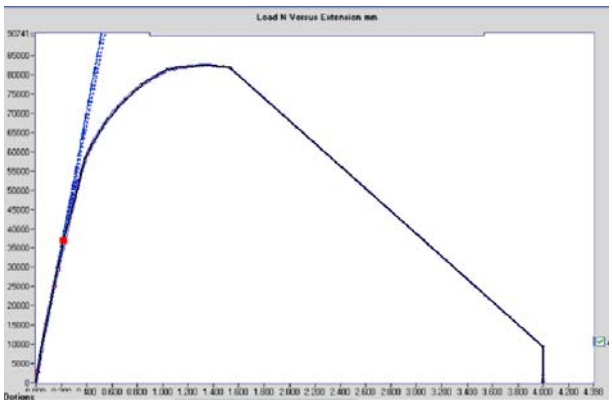

b) OLC45 – annealing

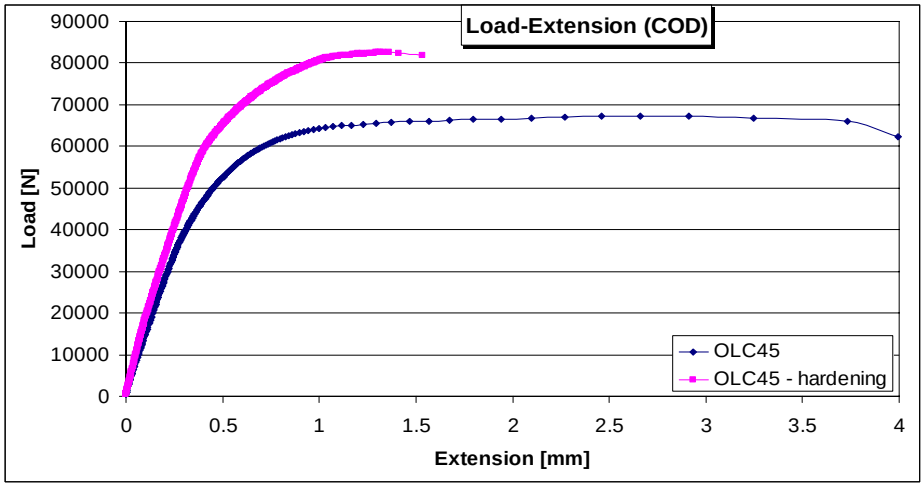

c) comparison between the curve for OLC45 and annealing OLC45

Fig. 7. Force-displacement curves.

Figure 7 presents the force-displacement curve for the tensile loading of the compact specimen made of OLC45, while fig. 7b presents the force-displacement curve for OLC45 annealing. In fig. 7c, in which the two curves are overlapped, we observed a difference between the allures of the two curves, with the fracture force values higher

for OLC45 annealing.

After the test took place, the KIc program exports the following data:
- The FQ force is automatically determined by the program, as in figures 7a and 7b, at the intersection of the force-displacement curve with the line at a 5% degree angle reported to the elastic portion: FQ-OLC45=25.59 kN, FQ-OLC45-annealing=36.85 kN,
- Fracture toughness KQ, which becomes KIc if test no validity problems occur.

Fracture toughness KQ is determined based on the following relations, for the sample loaded at tensile, [7]:

$$K_Q = F_Q \frac{f\left(\frac{a}{W}\right)}{BW^{\frac{1}{2}}} \tag{4}$$

where:

$$f\left(\frac{a}{W}\right) = 29.6\left(\frac{a}{W}\right)^{\frac{1}{2}} - 185.5\left(\frac{a}{W}\right)^{\frac{3}{2}} + 655.7\left(\frac{a}{W}\right)^{\frac{5}{2}} - 1017\left(\frac{a}{W}\right)^{\frac{7}{2}} + 638.9\left(\frac{a}{W}\right)^{\frac{9}{2}} \tag{5}$$

After the calculation of K_Q, we verify whether:

$$B, a \geq 2.5\left(\frac{K_Q}{\sigma_c}\right)^2 \tag{6}$$

For our case, the loaded samples had a B=25 mm thickness and a≈24 mm crack length.

For OLC45 we have $2.5\left(\frac{K_Q}{\sigma_c}\right)^2 = 15.44$ mm <B,a, while for the OLC45 annealing we have:

$$2.5\left(\frac{K_Q}{\sigma_c}\right)^2 = 20.02 < B, a$$

As a consequence, the validity condition (6) is fulfilled and the critical value of the intensity factor of the K_{Ic} load is considered to be equal to the value of the intensity factor of the K_Q load, so:

$$K_{Ic} = K_Q \tag{7}$$

For the samples made of OLC 45 and OLC45 annealed, the values for the fracture tenacity were:

$$(K_{Ic})_{OLC45} = 53.62\ \text{MPa}\sqrt{\text{m}} \quad \text{and} \quad (K_{Ic})_{OLC45\text{-calit}} = 42.06\ \text{MPa}\sqrt{\text{m}}$$

We can establish the character of the fracture by looking at the fracture surface of the specimen. The appearance of the fracture is an additional info and should be underlines for each sample. Figure 8 presents the appearances of the fracture surfaces for the two cases. We observe a significant deformation for the OLC45 sample, underlined by the deformation of the lateral sides of the fracture surface. The differences regarding the appearance of the fracture area are obvious: the initial area of the fissure (by fatigue), the slow-propagation area of the fissure under static tensile and the sudden-fracture area. For the OLC45 annealing sample we observed that the sudden-fracture area is inside the material, at a certain distance from the opposing notch.

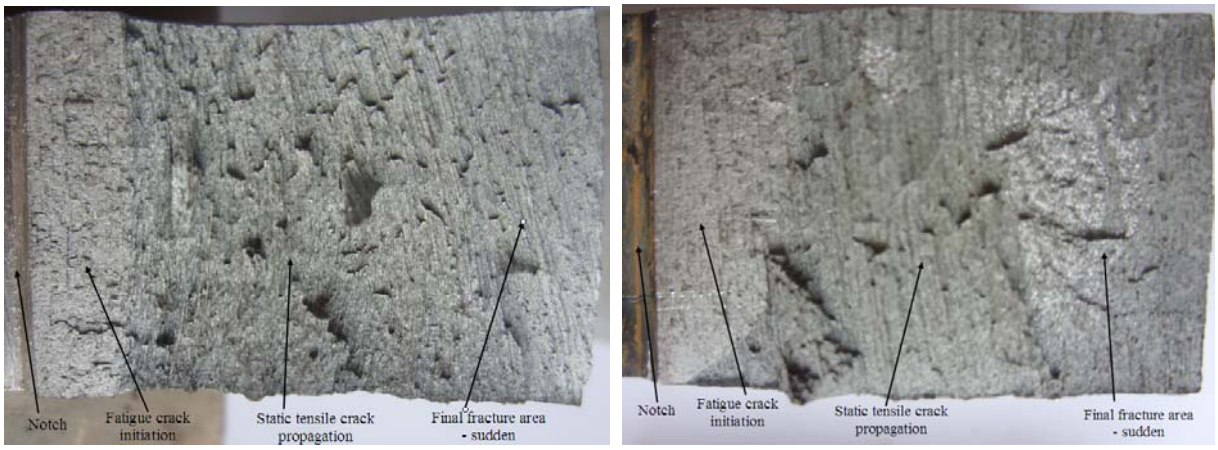

a) OLC45 – static (KIc) b) OLC45 annealed – static (KIc)

Fig. 8. The appearance of the fracture surfaces.

4. THE VICKERS MICRO-HARDNESS TESTS

As we can see from figure 8, the fracture of the surfaces of the compact samples happened due to pre-cracking by fatigue and afterwards due to the static loading for the K_{Ic} determination. On the whole surface, the appearance of the fracture is different. As a consequence, the processes that led to the fracture and plastic deformation in certain area are different. A simple, efficient and low-cost solution for establishing the level of plastic deformation suffered by a material is the hardness test.

It is a known fact that the value of hardness increases while the material experiences heavier plastic deformation [9, 10]. Based on the observation and considering the fact that there are various deformation areas on the fracture surface of the compact specimen, we used Vickers indentation as a method to determine the plastic deformation in various areas of the fracture surface, [11]. The indentations were made in the vicinity of the fracture surfaces, on the lean-surface side, as in Figure 9, because it was hard to observe the traces of the indentation on the fracture surface.

Starting from the notch, two rows of indentation were made along the fracture surfaces. Indentations were also made on a perpendicular direction reported to the fracture surface.

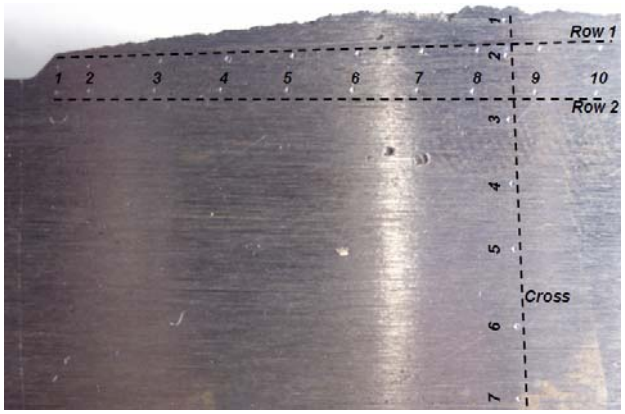

Fig. 9. Vickers indentations along the fracture surfaces.

The micro-hardness values were determined using an EMCOTEST M1C01A micro-hardness, with features such as data import, viewing and measuring of traces on the computer screen. In the graphs in Figure 10 variations of the Vickers micro-hardness values (the two rows for OLC45 – HV30 and OLC45 annealed – HV10) are presented.

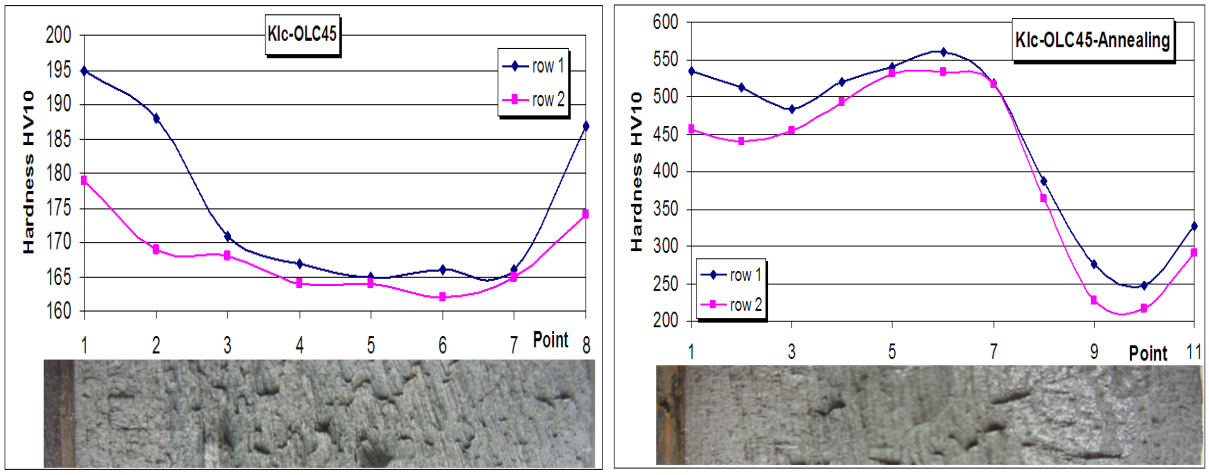

a) OLC45 – static (KIc) b) OLC45 annealed – static (KIc)

Fig. 10. The variation of the Vickers micro-hardness along the fracture surfaces.

From analyzing the graphs in Figure 10a, drawn for OLC45 steel, we observed that:

- In the area of the plastic deformation which appeared due to fatigue loading (initiated in order for the crack to appear) the micro-hardness values are higher;
- In the area of static loading, the rate of the loading is constant. Accordingly, in this area, a constant range of minimal values is established;
- The Vickers micro-hardness increases in the final area of the crack, where the propagation speed of the crack is higher;
- We observed that the value of the micro-hardness is lower on the second row of determination, which leads to the conclusion that, while we get further away from the fracture area, the plastic deformation gets lower.

By observing the graphs in Figure 10b, drawn for annealed OLC45 steel, we could draw the following conclusions:

- No significant differences appear, regarding the values of the micro-hardness between the area of the crack initiated due to fatigue and the area of the crack propagated by static tensile loading;
- Compared to the variation in this area, which we observed at OLC45 steel, the plastic deformation suffered as a consequence of the crack initiation due to fatigue is heavier than for the annealed OLC45 steel;
- The micro-hardness value decreases in the area containing the core with the larger, bright grains, representing a sudden detachment of the surfaces;
- An increase in micro-hardness takes place in the area of the final fracture, where the propagation speed of the crack is higher.

A comparison between the values of the Vickers micro-hardness, determined on row 1, at the same distance from the fracture surface, for both cases, may be seen in Figure 11a. We observed that the values of the Vickers micro-hardness are much higher than for annealed OLC45 steel, compared to OLC45.

Figure 11b presents the variation curves of te Vickers micro-hardness on a perpendicular direction on the fracture surface, as presented in Figure 11 (cross). In both cases, a decrease of the Vickers micro-hardness values may be observed, while we get further away from the fracture surface.

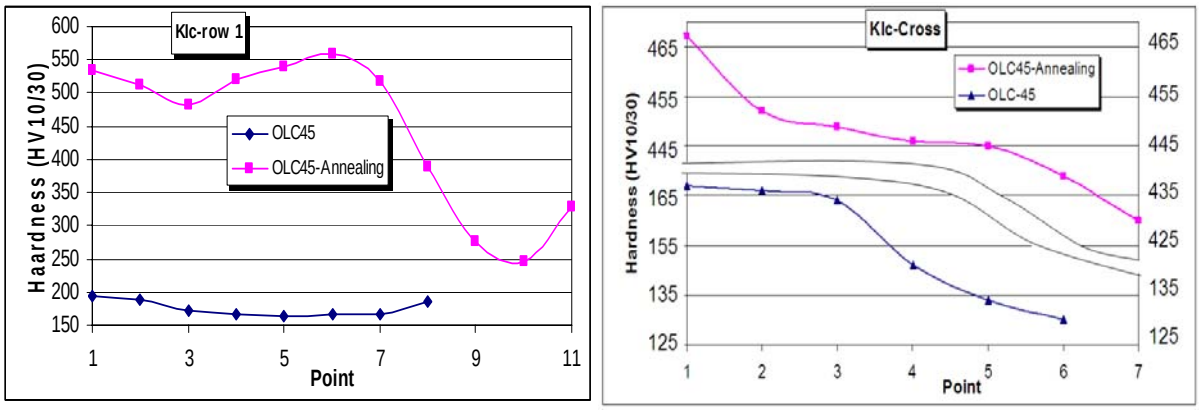

a) b)

Fig. 11. a) Hardness: OLC45+OLC45-annealing; b) Cross hardness: OLC45+OLC45- annealing.

5. CONCLUSIONS

In order to determine the fracture toughness, according to ASTMA E399, we used a compact specimen loaded at static tensile. The before mentioned standard requires that, before the static loading, the compact specimen to be loaded to fatigue loadings in order to initiate a crack in the notch. By analyzing the fracture sample, we observed areas with a different surface appearance. This also results from the fact that the mechanisms to propagate the crack on the fracture surface are different and, as a consequence, the level of plastic deformation changes accordingly. As we already mentioned, one of the methods to assess the level of plastic deformation is the micro-hardness test [12]. In this paper, we considered two test scenarios: for normal OLC45 steel, as delivered by the manufacturer, and annealed OLC45 steel.

By doing Vickers indentations along the fracture surfaces (resulted from loads used to determine K_{Ic}), we observed that different values are recorded in areas with different fracture appearances. As a result, we observed that values of the micro-hardness are higher in the place where the crack resulted due to fatigue was propagated. This is obvious for the normal OLC45 steel, while it is not as notable for the annealed OLC45. So, for the OLC45, the micro-hardness, while for the annealed OLC45 it is constant. For both cases, however, we observed an increase of the micro-hardness in the area of the final crack, where the crack propagation speed is higher.

As a following, the micro-hardness tests underlines the level of plastic deformation suffered by the material in the vicinity of an area where a crack was propagated, based on various techniques.

REFERENCES

[1] Kim, J. Y., Kang, S. K., Greer, R. J., Kwon, D., Evaluating plastic flow properties by characterizing indentation size effect using a sharp indenter, Acta Materialia 56, 2008, p. 3338–3343.
[2] Liu, Z., Harsono, E., Swaddiwudhipong, S., Material characterization based on instrumented and simulated indentation tests, International Journal of Applied Mechanics, Vol. 1, No. 1, 2009, p. 61–84.
[3] Tabor, D., The Hardness and Strength of Metals, Oxford Clarendon Press, 1951.
[4] Tabor, D., A Simple Theory of Static and Dynamic Hardness, Proc. Royal Soc. Series A., 192, 1947, p. 247-274.
[5] Dannenmann, E., Wilhelm, H., Steck, E., Uber den Zusammenhang zwishen Eindring-harte und Umformgrad bei Kaltumformvorgangen, Bander Bleche Rohre, 1968, p. 368-394.
[6] ***., EN ISO 6892 -1:2009, Tensile Testing of Metallic Materials.
[7] ***., ASTM E399 - 09e2, Standard Test Method for Linear-Elastic Plane-Strain Fracture Toughness KIc of Metallic Materials.
[8] ***. Instron FastTrack Software, K_{IC} Fracture Toughness Program, Reference Manual - Software, M22-10020-EN, Revision F.
[9] Jayaraman, S., Hahn, G.T., Oliver, W.C., Rubin, C.A., Bastias, P.C., Int Journal Solids Structures, 35, 1998, p. 365.

[10] Dao, M., Chollacoop, N., Van Vliet, K. J., Venkatesh, T. A., Suresh, S., Computational, modeling of the forward and reverse problems in instrumented sharp indentation, Acta Materialia, 49, 2001, p. 3899–3918.
[11] Chollacoop, N., Ramamurty, U., Simulation of deformation fields underneath Vickers indenter: Effects of power-law plasticity, J. Sci. Technol. 32 (2), Mar. - Apr. 2010.
[12] Goanta, V., Mares, M., Leitoiu, B., The evaluation of plastic strain level, for certain material, using the Vickers hardness test, ICSAAMM 2009 Conference, Tarbes, France, 7-10 sept. 2009.